Wood Science and Technology
https://doi.org/10.1007/s00226-024-01548-z

ORIGINAL

Characterisation of hygroelastic properties of compression and opposite wood found in branches of Norway spruce

Marie Hartwig-Nair[1] · Sara Florisson[1] · Malin Wohlert[1] · E. Kristofer Gamstedt[1]

Received: 26 July 2023 / Accepted: 22 March 2024

Abstract

The differential swelling seen between softwood opposite wood (OW) and its neighbouring compression wood (CW) developed in branches prompts several engineering issues such as dimensional instability and cracking. For a more efficient use of resources, the inevitable CW and OW should not be discarded or used as fuel, but incorporated into engineered wood products. Swelling is a hygroelastic phenomenon, where both the swelling and elastic properties of CW and OW are needed in order to make proper structural predictions. In this paper, swelling coefficients and moisture dependent elastic moduli for both CW and OW in the three principal material directions are provided along with measurements of moisture content, density, and microfibril angle. The small deformations necessitate the use of precise X-ray micro-computed tomography for measurements. The results indicate that CW and OW from Norway spruce branches differ in swelling, especially in longitudinal direction at low moisture content. It is noted that CW is a wood type with less pronounced anisotropic behaviour than both OW and normal wood from the stem, with the elastic moduli less sensitive to moisture changes in both longitudinal and transverse directions.

✉ E. Kristofer Gamstedt
kristofer.gamstedt@angstrom.uu.se

Marie Hartwig-Nair
marie.hartwig@angstrom.uu.se

Sara Florisson
sara.florisson@angstrom.uu.se

Malin Wohlert
malin.wohlert@angstrom.uu.se

[1] Applied Mechanics, Department of Materials Science and Engineering, Uppsala University, Box 35, SE-75103 Uppsala, Sweden

Published online: 16 April 2024

Introduction

Most of the timber used in engineered wood products originates from the stem of the tree. A material often overlooked, but of great potential, is wood from branches, which make up nearly 20% of the trees' biomass (He et al. 2018). However, branches are usually not further processed, except for fuel in energy production, at best. Nevertheless, from a zero-waste perspective and optimal use of material, the timber industry is looking for alternative ways to use the entire tree in the production of engineered wood products, rather than only stem wood. Apart from Olarescu et al. (2022), analysing panels made out of beech branches and minor spruce trees, this possibility has to the authors' knowledge been sparsely explored.

Compression wood is found in both stem and branches of conifers. Norway spruce stem wood consists mainly of normal wood (NW), but between 9% and 18% is stem compression wood, referred to as sCW in this paper. Within cross sections of Norway spruce branches, the lower side comprises branch compression wood, in the following denoted CW, whereas the upper side mostly opposite wood (OW), which is comparable to NW, as shown in Fig. 1 (Timell 1986). In general, CW is known to be darker than NW and OW in its colour and it differs from NW and OW in several ways. The shape of CW tracheids is more circular with thicker cell walls. The CW cell walls lack a S3-layer and have a higher microfibril angle (MFA) in the S2 layer. Furthermore, CW contains less cellulose and more lignin. The lignin has a higher ratio of 4-hydroxyphenyl to guiacyl (H/G) lignin units. Also, the lignin is homogeneously distributed throughout the S2 layer in CW, while in OW mostly located in the middle lamellae (Färber et al. 2001; Timell 1986; Donaldson and Singh 2016; Gardiner et al. 2014; Li et al. 2014; Zhang et al. 2016). These differences in chemical composition and cell wall characteristics affect the hygroelastic properties of CW and OW in branches, which have been the subject of a limited number of investigations (Timell 1986; Gurau et al. 2008; Harris 1977; Perstorper et al. 2001; Burgert et al. 2004; Müller et al. 2006; Stanzl-Tschegg et al. 2011).

Wood interacts with moisture throughout its entire life cycle, obviously in its green state, but also from felling to reuse. Wood hygroscopicity and its tendency to dimensionally change upon altered moisture conditions give rise to many

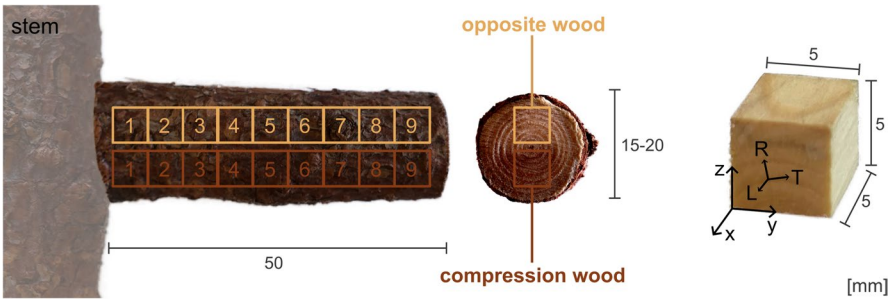

Fig. 1 Origin of the specimens from the tree branches. Example of specimen from OW used for experiments in this study

engineering challenges such as distortion and cracking. To promote the use of softwood branches, it is therefore necessary to characterise the hygroelastic properties of the branch wood constituents CW and OW and point out differences as well as similarities with NW.

Wood experiences shrinkage and swelling when desorbing or absorbing moisture below the fibre saturation point. When wood containing a combination of CW and NW or CW and OW is exerted to a change in moisture content (MC), large stresses may develop due to internal constraints caused by differential swelling or shrinkage in the different wood types. The dimensional changes that occur during the shrinkage or swelling process in the fibre direction of NW are usually small compared to the transverse directions. Bengtsson (2001) reports a moisture induced longitudinal swelling coefficient of 0.006, a radial swelling coefficient of 0.16 and a tangential swelling coefficient of 0.33. The changes in the tangential direction are about two times larger than those seen in radial direction, and 55 times larger than those seen in the longitudinal direction.

The longitudinal swelling or shrinkage coefficient of sCW is much higher than that of NW. The longitudinal shrinkage of sCW from green condition to oven-dry is between 0.71 and 3.58% (Timell 1986), while for NW it is between 0.09 and 0.47%. The radial and tangential shrinkage of sCW in percentage of green condition are between 2.11–2.72% and 3.15–3.40%, respectively. This can be compared to NW with values between 3.84 and 4.78% in radial and 6.53 and 9.30% in tangential direction respectively. The difference in longitudinal shrinkage seen between sCW and NW is caused by the large MFA in sCW. A large MFA facilitates longitudinal swelling and shrinkage and hampers the transverse changes, which reduces the degree of anisotropy (Boutelje 1973; Joffre et al. 2014; Perstorper et al. 2001; Purusatama et al. 2021). Similar shrinkage has been determined for branches of Norway spruce, with high longitudinal shrinkage seen in CW of 6.1%, in comparison to OW with a value of 0.5%. Radial and tangential shrinkage for CW were in a similar range with values of 3.1% and 3.7 %, respectively, while the value for OW was more than double as high with values of 7.8% and 8.8% (Timell 1986).

For stem wood of Norway spruce using compression tests, it was found that sCW has a lower elastic modulus than NW, with a value of 9.57 GPa compared to 11.14 GPa (Timell 1986). Branch wood has in general a lower elastic modulus than NW. For example, a 10% lower stiffness for CW than for NW was reported for several American conifer species by Timell (1986), while Gurau et al. (2008) found the stiffness of Scots pine CW to be even 75% lower than for NW. To the authors' knowledge, the stiffness of OW and CW in branches has not been explicitly investigated. Studies have also mainly focused on elastic properties in longitudinal direction.

To gain information about wood structure, computed tomography (CT)-scanning is nowadays a technology more commonly used in the sawmill industry. Micro-computed tomography (μCT) using X-rays has permitted even more detailed investigations of the shrinkage and swelling of wood with table-top laboratory based equipment (Badel and Perré 2001; Derome et al. 2011). X-ray μCT offers a technique to measure overall dimensional changes in 3D, significantly surpassing the precision of conventional techniques based on micrometer screws and calipers.

The method also reduces the impact of surface related uncertainties, which is rather common in moisture dependent experiments of wood (Withers et al. 2021).

The main objective of this paper is to characterise the hygroelastic properties of Norway spruce branch wood, divided into CW and OW, to allow more accurate predictions of its behaviour in construction and/or engineered wood products. A special focus is put on the determination of swelling coefficients using μCT and the moisture dependent elastic moduli in longitudinal and transverse directions. These values were supplemented with measurement of moisture content, density and MFA.

Materials and methods

CW and OW specimens were retrieved from Norway spruce branches to determine the swelling coefficients and moisture dependent elastic moduli at three different levels of relative humidity (RH) in the principal material directions. The swelling coefficients were determined by μCT and subsequent image analysis. The elastic moduli were obtained through compression testing. The tests were supplemented with measurements of MC, dry-density and MFA. The MFA was determined using wide-angle X-ray Scattering (WAXS) experiments. Variations due to age, location, species and environmental factors were not taken into account in this study. In the following sections the preparation of specimens, the experimental setup and post-processing of results are discussed.

Specimen preparation

Specimens were taken from six branches of a Norway spruce (*Picea abies* [L.] Karst.) tree located in Tranås, in southern Sweden. The diameter of the stem without the bark was 12.5 cm at 25 cm height, estimating the tree to an age of 30 years. The diameter of the branches closest to the stem was approximately 20 mm. All branches were taken at a height of approximately 30 cm. The branches were wrapped in plastic and frozen after felling. Before preparing the specimens, the branches were defrosted and stored at ambient climate (21 °C, 40–60% RH) for drying. The specimens were obtained from the 10 cm of the branch closest to the stem by a professional carpenter. Each branch was horizontally cut at the pith to separate CW and OW. The pronounced darker colour of CW was used to select specimens containing only OW or only CW. From each branch, three matching pairs of CW and OW from the same cross section were cut into cubes with an edge length of 5 mm. Only pairs, where both CW and OW were clear wood, were selected. This is shown in Fig. 1 and Table 1. In total, 18 specimens of each wood type were characterised both by hygroexpansion and mechanical testing at different levels of RH.

Conditioning of specimens

Since swelling was of interest, an absorption experiment was carried out by conditioning the specimens at a higher RH between each CT-scan, according to the

Table 1 Specimens selected from the branches for hygoexpansion and mechanical testing. Increasing number indicates the increased distance from the stem accoring to Fig. 1

	Branch 1	Branch 2	Branch 3	Branch 4	Branch 5	Branch 6
Opposite wood	2,3,4	3,4,5	1,2,3	1,2,3	2,3,4	1,2,3
Compression wood	2,3,4	3,4,5	1,2,3	1,2,3	2,3,4	1,2,3

levels in Table 2. After the absorption, the specimens were oven dried at 103 ± 2 °C according to standard SS-EN13183-1 (CEN 2003) to determine the oven-dry density. The specimens were again subjected to the same absorption for mechanical testing.

The specimens were conditioned in a desiccator with an over-saturated salt solution to obtain a certain RH at room temperature (approx. 20 °C) and accordingly an equilibrium MC in each specimen. In Table 2, the used salts, the obtained RH in the desiccator, and the expected equilibrium MC of the wood specimens are listed. The expected equilibrium MC was estimated using Simpson's equation for Sitka spruce (Simpson 1973). The specimens were successively left for conditioning in each climate for 48 h. The time required to reach the equilibrium MC was determined beforehand on dummy specimens. Temperature and RH were tracked with data loggers Comet Q-U3120 (COMET system, Rožnov pod Radhoštěm, Czech Republic). These loggers had a measurement range between −30 °C and +70 °C and a RH range between 0 and 100% with an uncertainty of ± 0.4 °C and ± 1.8% RH, respectively.

General characterisation

The oven-dry density, ρ_0, of each specimen was determined according to

$$\rho_0 = \frac{m_0}{V_0} \tag{1}$$

with m_0 being the oven-dry mass and V_0 being the oven-dry volume of the specimen. The mass of each specimen was measured with an analytical balance Mettler Toledo XS 105 ± 0.01 mg (Mettler Toledo, Columbus, USA). The dimensions of the specimen were measured with a digital caliper Cocraft 40–8747 ± 0.03 mm (Clas Ohlson, Insjön, Sweden).

Table 2 Conditioning of specimens in desiccator with different saturated salt solution and the resulting levels of relative humidity (RH) and moisture content (MC)

Saturated salt solution	RH at 20 °C (%)	Expected equilibrium MC (%)
Potassium carbonate	44	8.3
Sodium chloride	75	14.5
Potassium sulfate	98	26.6

The MC at the different RH levels, u_{RH}, was determined based on the oven-dry method (CEN 2003)

$$u_{RH} = \frac{m_{RH} - m_{0\%}}{m_{0\%}} \tag{2}$$

with the m_{RH} being the mass at a certain RH and $m_{0\%}$ being the mass of the oven-dry state.

Microfibril angle measurements

WAXS was chosen, since it allows efficient analysis of the average MFA of a specimen. This is important for understanding the mechanical properties. Andersson et al. (2000) and Donaldson (2008) reported good agreement with only little difference in MFA between X-ray diffraction and polarisation microscopy for Norway spruce.

The MFA was measured on 1 mm thick transverse slices (*zy*) taken from the centre of all specimens. The WAXS was performed at the synchrotron beamline ForMAX at MAX IV Laboratory, Lund, Sweden. The wavelength of the beam was 0.616 Å. The size of the incident beam was 0.9 mm × 1.2 mm. The calculated MFA is hence an average of all tracheids in this section as shown in Fig. 2. The MFA was calculated from the 004 reflection. This allows for a direct calculation of the MFA both for tracheids with round and rectangular cross-sections. Close by reflections were taken into account according to Andersson et al. (2000). It should be noted that the values presented here are not the MFAs of the dominant S2-layers, but an average over the entirety of the wood sample, including cellulose microfibril orientations also from the primary cell walls, middle lamellae, the S1-layes and, if present, the S3-layers.

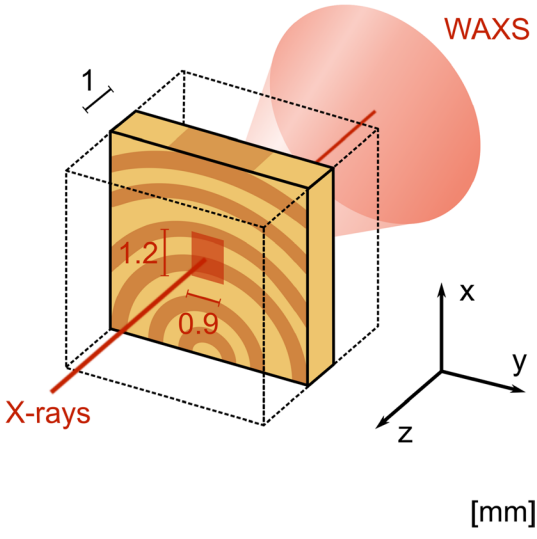

Fig. 2 Volume of original specimens (in red) analysed by wide-angle X-ray scattering (colour figure online)

Swelling properties

CT scanning

The specimens were scanned with a μCT-scanner Skyscan 1172 (Bruker, Kontich, Belgium). The system had a stationary X-ray source and detector, while the specimen was rotated. The instrument used a cone beam. During scanning, three specimens were stacked on top of each other and wrapped in foil to reduce the loss of moisture during the scanning time of approximately six hours. Settings for all scans are shown in Table 3. A flatfield correction including both bright and darkfield was carried out at the beginning of each day of scanning. The flatfield correction reduces artefact caused by the inhomogeneity of the X-ray beam, stationary noises at the detector and dust particles in the system. The reconstruction software NRecon (Bruker, Kontich, Belgium) was used to convert the 2D projections to cross-sectional slices.

Image analysis

The tomograms were analysed in software Fiji (Schindelin et al. 2012). Swelling was measured for three different material directions. The *z*-direction in the *yz*-plane, the *x*- and *y*- directions in the *xy*-plane. For each direction, 9 tomograms at a fixed distance from each other were analysed. In these tomograms one measurement per direction was carried out, as shown in Fig. 3. The length was always measured in the middle of the cube dividing it into two halves. The measurements of the 9 tomograms were averaged. To ensure measurement in the same position for all levels of RH, the tomograms were visually assessed and matched, which may have introduced a small error. Due to the analysis method, the swelling coefficients found in the *z*-direction coincides with the longitudinal material direction, the coefficients found in the *x*-direction are dominated by the radial material direction of the wood material, and the coefficients found in the *y*-direction are a combination of the radial and tangential directions defined by the annual ring curvature.

Table 3 Settings for μCT scanning

Variable	Setting
Pixel/voxel size	2.99 μm
Voltage	49 kV
Current	200 μA
Exposure time	750 ms
Averaging (frames)	4
Filter	non
Rotation step	0.2°
Total rotation	180°
Scanning time for stack (3 specimens)	approx. 6 h
Temperature	26–27°C

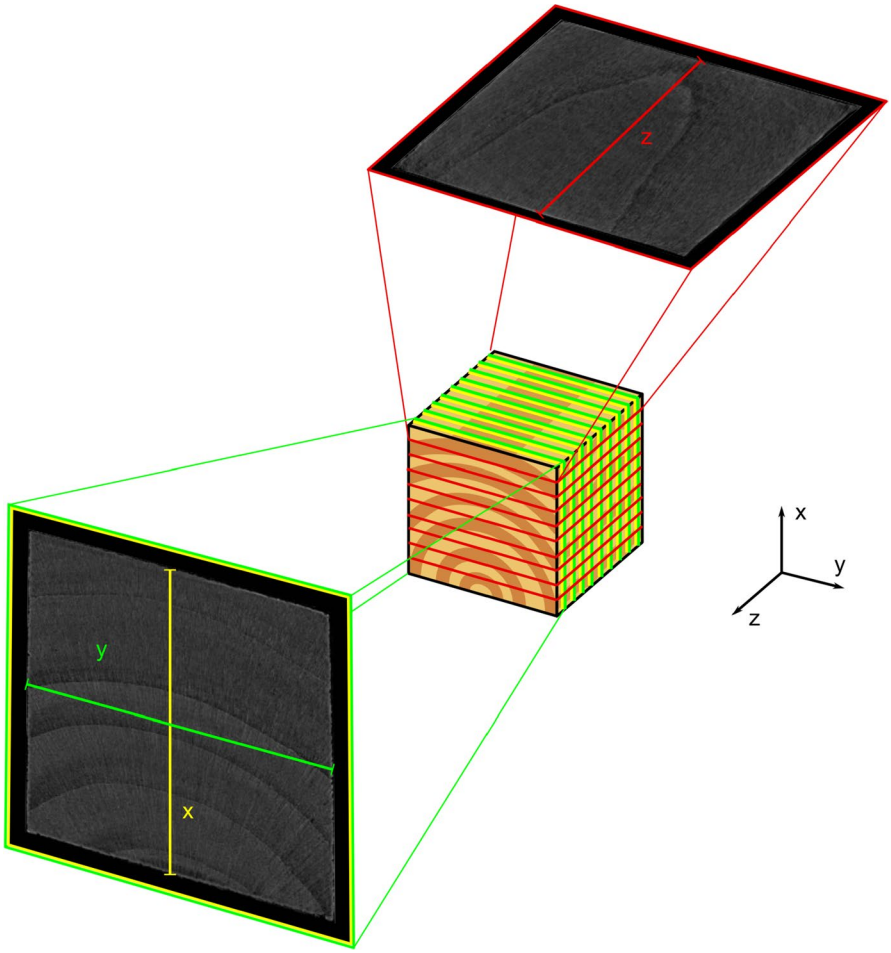

Fig. 3 Measurement of deformation in *x*- and *y*-direction in the *xy*-plane, and in *z*-direction in the *yz*-plane. Measurements for each direction were done in nine slices of the respective plane

Determination of swelling coefficient

The uniaxial strain due to hygroexpansion, ε, was based on the dimensions of the specimens at a RH of 44%, $h_{44\%}$:

$$\varepsilon = \frac{h_{\mathrm{RH}} - h_{44\%}}{h_{44\%}} \tag{3}$$

where h_{RH} indicates the dimension at either 75% or 98% RH.

Consequently, the uniaxial swelling coefficient α was also based on the dimensions and MC at a RH of 44%, viz.

$$\alpha = \frac{\varepsilon_{\mathrm{RH}}}{u_{\mathrm{RH}} - u_{44\%}}. \tag{4}$$

The strain and swelling coefficient were determined for all three directions (x, y and z) for all specimens. It should be noted that these are swelling coefficients. Shrinkage coefficients can have different values due to sorption hysteresis.

Elastic properties

Compression testing

Compression tests were applied to determine the elastic properties of CW and OW. A universal testing machine Shimadzu Autograph AGS-X (UTM: Shimadzu, Kyoto, Japan) was used with a 500 N load cell. The specimens were placed between two parallel plates, which were fixed in position and did not adjust to any non-parallelism in the specimen, which could lead to uneven compression. Therefore, the specimens were carefully machined by a professional carpenter using precision tools. Inevitably, during compression testing, the specimens could not expand freely due to Poisson effects in the perpendicular direction closest to the surface of the compression plates. This may cause a non-uniform multiaxial stress-state close to the supports instead of a uniform uniaxial situation, although this effect was considered small compared to the scatter in properties (Vorobyev et al. 2016). The displacement was measured with the digital video extensometer TRViewX Shimadzu (Shimadzu, Kyoto, Japan). This is a contact free measuring device with a relative accuracy of 0.5%. Since the specimens were small, the displacement of the loading plates, rather than the specimens, was measured. Optical measurement of the displacement of the plates reduces the effect of machine compliance. It also means that the average displacement was measured. The tests were carried out at a displacement rate of 0.5 mm/min. The sampling rate was 100 Hz. The choices made in the setup of the compression test and displacement measurement led to small errors in the determined elastic moduli. The specimens were tested and analysed in x-, y- and z-direction. A maximum stress was selected to ensure that the specimens just deformed elastically. The limit for the transverse directions x and y was set to 50 N and for the longitudinal direction z to 250 N, within the linear elastic regime.

Determination of elastic modulus

The elastic modulus E was determined as

$$E = \frac{\Delta F L_0}{A \Delta l} \tag{5}$$

with ΔF being the regarded interval in the applied load, L_0 being the height of the cube, A being the cross-sectional area of the loaded surface, and Δl being the regarded section of the displacement curve. The regarded section of the load-displacement curve for ΔF was between 30 and 40 N for the x and y-direction and between 150 and 200 N for the z-direction. Within these intervals, linear

load-displacement and stress–strain relations were observed. To calculate the elastic modulus, the data was smoothed by a moving average over 100 data points. Due to the testing procedure, the tested z-direction corresponds to the longitudinal direction in wood, while x and y are transverse directions whose properties are based on a combination of varying radial and tangential properties.

Statistics

Swelling coefficients, elastic moduli, density, MC and MFA were tested for normal distribution for a small number of specimens. The Shapiro-Wilk or the Shapiro-Francia test of normality was used depending on the kurtosis of the probability distribution. Since some of the data did not perfectly match a Gaussian distribution, this data was checked for equality of median through the Wilcoxon rank sum test for equality of median. The significance level α for all tests was 0.05, so that the tests are sensitive enough for the small sample size, but limiting the risk of false positive.

It was chosen to represent the data in boxplots, where the centre line of the box corresponds to the median. The box is defined by the first and third quartile and its width is expressed as the interquartile range (IQR). The whiskers mark the minimum and maximum value of the data set excluding the outliers. Outliers are defined as values in the data set which are 1.5 times the IQR away from the first or third quartile.

Results and discussion

In the following section, the determined swelling coefficients, elastic properties, MC and density for each RH and for both the CW and OW are presented.

Density and moisture content

In Fig. 4 and Table 4, the oven-dry density and MC of both CW and OW are presented. The oven-dry density of OW and CW is 797 kg/m^3 and 880 kg/m^3, respectively. Both are much higher than the average density of NW of Norway spruce, usually reported to be around 400 kg/m^3 (Dahl and Malo 2009; Dinwoodie 2017). This observation is in agreement with previously reported observations of specific gravity of CW being higher than of OW (Timell 1986). Also, Hakkila 1969, 1971 (summarised by Timell (1986)) reported high densities for branch wood, especially when located closest to the stem. Values as high as 890 kg/m^3 were reported. The high density of both OW and CW can be attributed to both wood types having cross sections with high cell wall to lumen ratio. Their cell micro structures also differ, where OW has rectangular shaped tracheids changing to circular cross sections in CW (Tarmian and Azadfallah 2009).

The moisture uptake is not the same for CW and OW. At 44% RH, the median MC in CW of 10.9% is significantly higher than that of OW with a value of 9.7%. This was also observed by Zhan et al. (2021), who reported higher MC in sCW

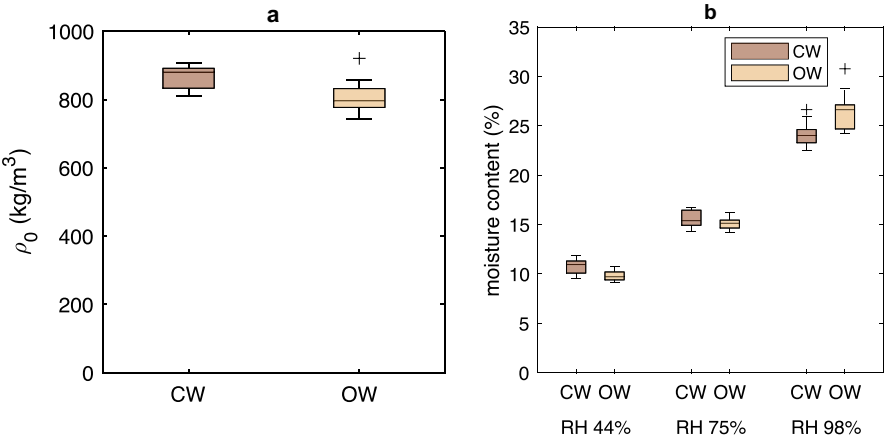

Fig. 4 Oven-dry density (ρ_0) of CW and OW (**a**). Moisture content (MC) of the specimens at the three different RH levels (**b**)

Table 4 Oven-dry density (ρ_0) and moisture content (MC) presented as median (M) and interquartile range (IQR)

	ρ_0 in kg/m^3		MC in %					
			44% RH		75% RH		98% RH	
	M	IQR	M	IQR	M	IQR	M	IQR
OW	797	55	9.7	0.8	15.2	0.8	26.6	2.4
CW	880	58	10.9	1.2	15.4	1.5	24.0	1.3

compared to NW. They suggest that differences in the distribution of hemicellulose and lignin between the microfibrils contribute to this phenomenon. However, the opposite is measured at 98% RH, where the median MC in CW of 24.0% is significantly lower than OW with a value of 26.6%. Since lignin is the most hydrophobic non-crystalline component in wood, a reason for the lower values can be the higher lignin content in CW and the different lignin distribution in CW cell walls. Furthermore, at molecular level, more 4-hydroxyphenyl (H) lignin units and less guaiacyl (G) lignin units are present in CW, and hence less methoxy functional groups (Donaldson and Singh 2016). This may affect the moisture uptake. However, more research is needed to understand the interaction between lignin and water, and the properties of hydrated lignin together with cellulose and hemicelluloses inside the cell wall.

Microfibril angle

In Fig. 5 the average MFA of CW and OW is presented. The predominant MFA in the cell wall in CW has a median value of 53° together with another MFA angle of 89°, also found in CW. The median MFA in OW is 41°. Between CW and OW, the

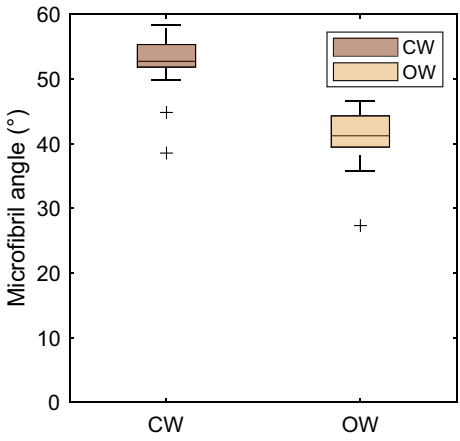

Fig. 5 Predominant microfibril angle in the cell walls of several tracheids measured by wide angle X-ray scattering

predominant MFAs differ significantly. In general, high MFAs in branch wood have been observed, with an MFA of 30–35° for OW and 40–45 ° for CW (Färber et al. 2001; Reiterer et al. 1998; Timell 1986). Färber et al. (2001) found that the MFA closest to the stem, as in this study, is particularly high and can range between 40° –50° in CW and 30°–40° in OW, depending on the considered annual ring. The high MFA in combination with the increased density have been shown to lead to higher fracture toughness needed to handle the loads that the tree branch is subjected to (Jungnikl et al. 2009).

Swelling properties

The swelling coefficients for the *z*-direction are shown in Fig. 6 and for the *x*- and *y*-directions in Fig. 7. The median and IQR are separately listed in Table 5. It is observed that the swelling coefficient of CW in *z*-direction is significantly higher than for OW. The median swelling coefficient for CW is 0.246 at RH 98%, while for OW a value of 0.020 is found at the same RH. Despite the difference being slightly less at RH 75%, the swelling coefficient of CW in the *z*-direction is still 10.7 times higher than for OW. These observations are in concordance with previous studies. For example, Timell (1986) reported longitudinal shrinkage that was nearly four times higher for NW than for stem CW in Norway spruce. Furthermore, Boutelje (1966) found the longitudinal shrinkage in branches of Norway spruce to be at least 10 times higher in CW than in OW (Timell 1986). The determined swelling coefficients do not differ significantly between a RH of 75% and 98%. Higher longitudinal shrinkage is attributed to the higher MFA in CW (Färber et al. 2001). However, it has also been suggested that other polymers such as lignin and highly swellable (1⟶3)-β-D-glucans in the cell wall are contributing to the distinct swelling behaviour of CW (Leonardon et al. 2010). This could be corroborated by the finding of low or negative swelling in OW, even though the MFA is high in OW close to the stem (approx. 30°)(Färber et al. 2001; Timell 1986).

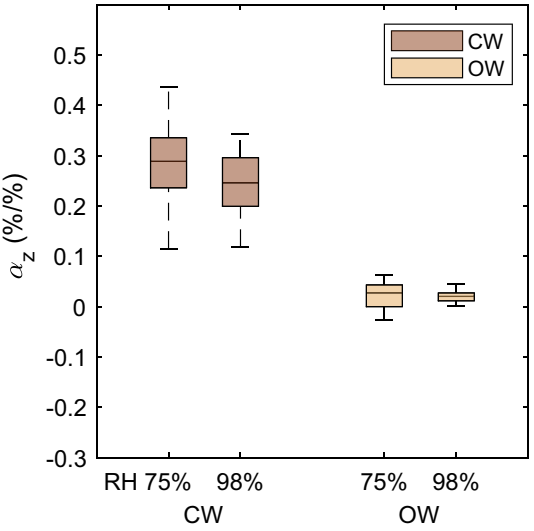

Fig. 6 Swelling coefficient (α) based on dimensions at a relative humidity of 44% in z-direction (longitudinal) for different levels of relative humidity

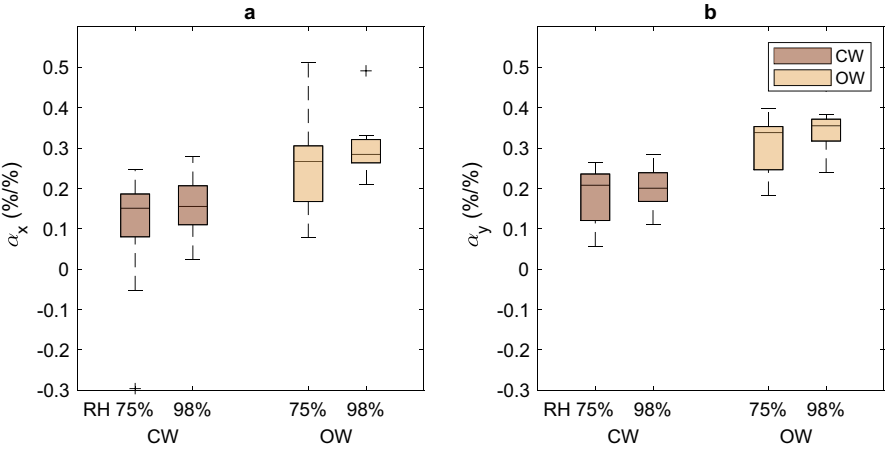

Fig. 7 Swelling coefficient (α) based on dimensions at a relative humidity of 44% in x-direction (radial) and y-direction (transverse dominated by tangential) for different levels of relative humidity

In the x and y-directions, the median swelling coefficient of OW at RH 98% are 0.267 and 0.338 respectively. The swelling coefficient of CW follows the same trend, but is overall smaller than for OW, being 0.151 and 0.208, respectively. The swelling coefficients in x- and y-direction differ slightly. As mentioned in the Material and Methods section, the x-direction coincides with the radial direction, while the y-direction is a combination of radial and tangential direction. Due to the curvature of the annual rings in the specimens, the measured swelling in y-direction is therefore dominated by swelling in tangential direction with a non-negligible contribution of radial swelling. To obtain the tangential swelling coefficient, a numerical

Table 5 Swelling coefficients (α) based on specimen dimensions at a relative humidity of 44% and elastic moduli (E) for different levels of relative humidity and material directions presented as median (M) and interquartille range (IQR)

	α in %/%				E in MPa					
	75% RH		98% RH		44% RH		75% RH		98% RH	
	M	IQR	M	IQR	M	IQR	M	IQR	M	IQR
z-direction										
OW	0.027	0.043	0.020	0.016	1263	750	1227	177	747	219
CW	0.289	0.099	0.246	0.097	914	351	784	330	667	183
x-direction										
OW	0.267	0.138	0.284	0.058	362	143	315	135	250	85
CW	0.151	0.106	0.156	0.097	461	259	400	235	313	142
y-direction										
OW	0.338	0.107	0.355	0.054	251	65	253	199	211	41
CW	0.208	0.115	0.201	0.071	347	210	370	189	322	129

approach as presented by Florisson et al. (2023) can be chosen. Higher tangential swelling and shrinkage in softwood branches has been described by Boutelje (1966), and for sCW and NW by Timell (1986). Perstorper et al. (2001) reported higher tangential than radial shrinkage in sCW of Norway spruce. In spite of the *y*-direction not being purely tangential, the obtained coefficients suggest that tangential swelling is higher than radial swelling in branches. Also, these swelling coefficients do not differ significantly between a RH of 75% and 98%. However, the range between the extreme values, when excluding outliers, is much larger for 75%. This suggests that assessing the swelling for a higher increase in MC might lead to more precise results. Differences in dimensional changes in the radial and tangential directions due to variations in MC will have implications in crack development during drying of branch wood.

Elastic properties

In addition to the presented swelling coefficients, elastic moduli at different levels of RH were measured for CW and OW in branches. The results for the *z*-direction are shown in Fig. 8 and for the *x*- and *y*-directions in Fig. 9. The median and IQR are separately listed in Table 5. In Fig. 8 it is shown that the longitudinal elastic modulus (E_z) is higher in OW than CW at all selected levels of RH. For instance, at a RH of 44%, the elastic modulus of OW is 1.26 GPa and of CW is 0.91 GPa. At a RH of 75%, the difference is even more prominent with a value of 1.23 GPa and 0.78 GPa for OW and CW, respectively. These elastic properties are small compared to the elastic modulus of NW found in Norway spruce with average values around 11 GPa. In addition, Gurau et al. (2008) found for Scots pine that the modulus of elasticity (MOE) of branch wood is only a quarter of the MOE of stem wood, with values of 3.32 GPa and 11.71 GPa respectively. In that study, no distinction was

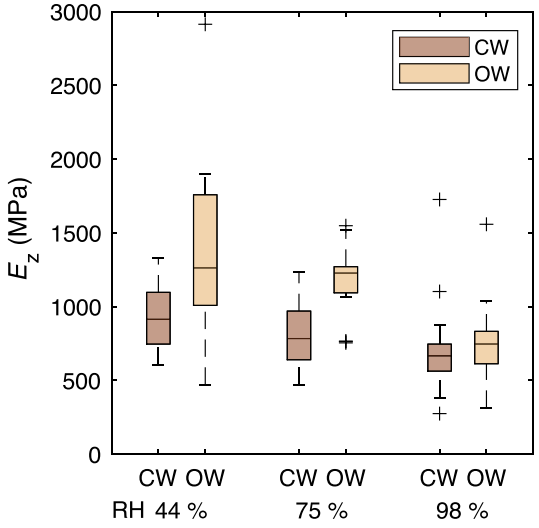

Fig. 8 Elastic modulus (E) at different relative humidity levels in z-direction (longitudinal)

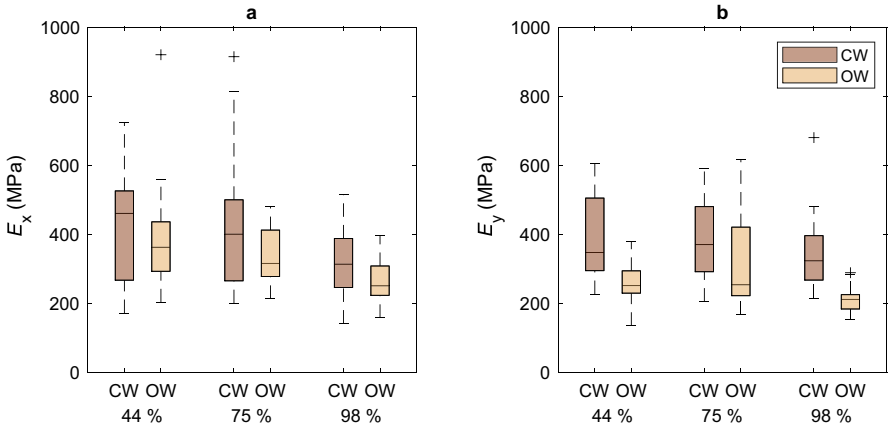

Fig. 9 Elastic moduli (E_x and E_y) at different relative humidity levels in x-direction (transverse dominated by radial) and y-direction (transverse dominated by tangential)

made between CW and OW in the branch. Similar results were found for various conifer species, even though the difference was not as extreme. Values for the MOE of 6.99 GPa were found in the stem and values of 6.29 GPa in the branch. For a variety of species, among them Norway spruce, a lower elastic modulus has been observed for CW when tested in compression (Timell 1986).

Färber et al. (2001) showed that the MFA in OW close to the stem is high in comparison to NW, and that the MFA of CW found in branches is even higher. Since the stiff cellulosic microfibrils are the main contributors to the cell wall stiffness, the MFA has a high impact on the cell wall longitudinal stiffness. This can be an explanation for the rather big difference found in stiffness between NW and branch

wood, and the less pronounced difference between CW and OW found in branches. However, the relatively small differences in MFA seen between OW and CW (10°) still impact the elastic modulus significantly.

The transverse elastic modulus in x and y-directions (E_x and E_y) of both OW and CW is presented in Fig. 9. It tends to be higher in the x-direction than in the y-direction, without being significantly different. Depending on the RH, the elastic modulus ranges between 250 MPa (RH 98%) and 461 MPa (RH 44%) for the x-direction, while it is between 211 MPa (RH 98%) and 347 MPa (RH 44%) for the y-direction. Norway spruce NW is usually stiffer in radial than in tangential direction (Keunecke et al. 2008). Considering that the x-direction is dominated by the radial direction and y-direction by the tangential direction, the results confirm previous findings. The elastic modulus of CW in x-direction is rather high, with a value of 461 MPa at RH 44 %. This could be caused by the high MFA as well as the difference in chemical composition of cell wall compared to OW. Bergander and Salmén (2002) concluded from simulations made at cell wall level that the transverse modulus is not only influenced by the properties of the S2-layer (MFA and thickness), but also the properties of hemicellulose and lignin. Cell wall behaviour may then be understood from composite mechanics, where the high stiffness of fibres dominates the longitudinal direction, and the lower stiffness of the matrix plays a larger role in the transverse direction.

A decrease in stiffness due to an increase in MC was observed for both types of wood and all three directions of testing. This is shown in Figs. 10 and 11 with the help of a linear regression analysis for both CW and OW. In general, the elastic modulus decreases with an increasing MC (Dinwoodie 2017). Outstanding in this case is the rather weak decrease in longitudinal stiffness for CW. This indicates that in longitudinal direction the stiffness is less dependent on the MC, which is a helpful characteristic from an engineering perspective. However, the rather high

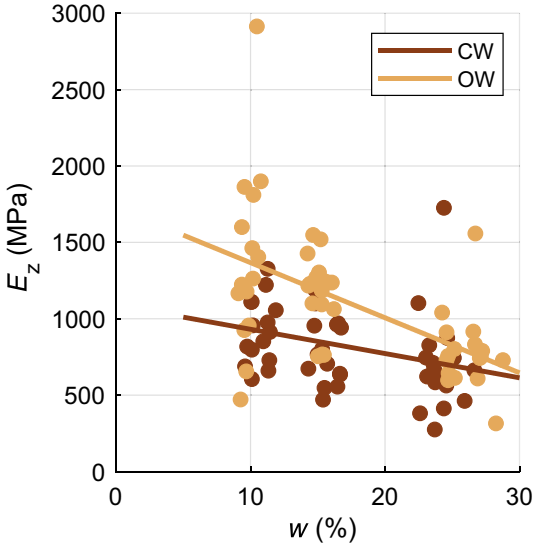

Fig. 10 Elastic modulus (E) as a function of moisture content in z-direction (longitudinal). Linear regression lines are presented for CW and OW

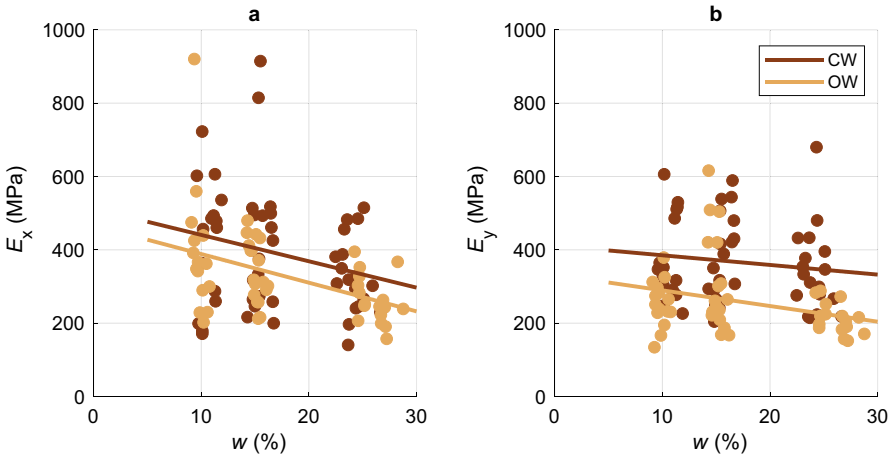

Fig. 11 Elastic modulus (E) over moisture content in x-direction (transverse dominated by radial) and y-direction (transverse dominated by tangential). Linear regression for CW and OW

longitudinal swelling should also be noted for possible future engineering applications, where the differential swelling could influence the dimensional stability of wood-based materials.

The decrease in stiffness is not as pronounced in x and y-direction. The regression lines are nearly parallel to each other and relatively flat, indicating that elastic moduli are neither affected by the differences between CW and OW, nor the MC. Important to notice is that the linear regressions have a poor goodness of fit as shown in Table 6. Hence the results should be interpreted as a trend, but not as statistically significant.

No significant correlation was found between the elastic modulus and density. This was already shown for the same material by Florisson et al. (2023). A probable reason for the lack of correlation is that the variability in density was rather small combined with a scatter in the elastic modulus.

Table 6 The slope, intercept and goodness of fit R squared (R^2) for linear regressions of elastic moduli of compression wood (CW) and opposite wood (OW) for z, x and y

	z		x		y	
	CW	OW	CW	OW	CW	OW
Slope	−15.88	−36.06	−7.19	−7.81	−2.63	−4.27
Intercept	1090	1728	513	467	412	332
R^2	0.11	0.31	0.06	0.20	0.02	0.10

Conclusion

In the present study, important hygroelastic properties for OW and CW in branches of Norway spruce are provided. Swelling coefficients and elastic moduli are compiled in longitudinal (z), radial (x) and tangentially dominated (y) directions of cubical specimens of CW and OW at different RH levels, supplemented with information about density, MC and MFA.

CW is found to swell 11–12 times more in longitudinal direction compared to OW at all levels of RH. On the contrary, OW shows approximately two times higher swelling than CW in its transverse directions. In fact, CW has swelling coefficients in the same order of magnitude in all measured directions. Both branch wood types (OW and CW) show lower elastic moduli than NW, especially in the longitudinal direction. The results clearly reveal that increasing MC affects the longitudinal elastic modulus (E_z) of CW less than E_z of OW.

The density of both CW and OW is found to be significantly higher than NW density, and density of the CW specimens is in turn higher than that of OW specimens. The moisture uptake differs between CW and OW. CW has a higher MC than OW at a RH of 44%, while it has a lower MC at a RH of 98%. The predominant MFA in the cell wall of the tracheids is 29% higher for CW than OW.

In summary, the results indicate that CW from Norway spruce branches is a wood type with less pronounced degree of swelling anisotropy than both OW and NW, and with elastic moduli less sensitive to moisture change in all material directions than OW. This knowledge can facilitate the use of branch wood in engineering applications, where high stiffness is not needed, but rather moisture stability and similar properties in longitudinal and transverse directions. The observed differences in moisture-induced deformations and stiffness for the branch wood tissues will affect the risk of cracking and dimensional instability of wooden products containing branch wood materials.

Acknowledgements This research has been funded by the Swedish Research Council, Grant 2016-04534. We thank Mr. Corentin Briot for able assistance in the CT-scanning and image analysis.

Author Contributions Conceptualization: Marie Hartwig-Nair (MH), Kristofer Gamstedt (KG), Malin Wohlert (MW), Sara Florisson (SF); Methodology: MH, KG, MW; Validation: MH; Data curation: MH; Formal analysis and investigation: MH, SF; Writing—original draft: MH; Writing—review and editing: MH, SF, MW, KG; Visualization: MH; Funding acquisition: KG; Resources: MW; Supervision: KG, MW, SF; Project administration: MH.

Funding Open access funding provided by Uppsala University.

References

Andersson S, Serimaa R, Torkkeli M, Paakari P, Saranpää P, Pesonen E (2000) Microfibril angle of Norway spruce [Picea abies (L.) Karst.] compression wood: comparison of measuring techniques. J Wood Sci 46(5):343–349. https://doi.org/10.1007/BF00776394

Badel E, Perré P (2001) Using a digital X-ray imaging device to measure the swelling coefficients of a group of wood cells. NDT &E Int 34:345–353. https://doi.org/10.1016/S0963-8695(00)00072-4

Bengtsson C (2001) Variation of moisture induced movementsin Norway spruce (*Picea abies*). Ann For Sci 58(5):568–581. https://doi.org/10.1051/forest:2001146

Bergander A, Salmén L (2002) Cell wall properties and their effects on the mechanical properties of fibers. J Mater Sci 37:151–156. https://doi.org/10.1023/A:1013115925679

Boutelje J (1973) On the relationship between structure and the shrinkage and swelling of the wood in Swedish pine (Pinus silvestris) and spruce (Picea abies). Svensk papperstidning 2:78–83

Boutelje JB (1966) On anatomical structure moisture content density shrinkage and resin content of wood in and around knots in swedish pine (pinus silvestris l) and in swedish spruce (picea abies karst). Svensk Papperstidning-Nordisk Cellulosa 69(1):1

Burgert I, Frühmann K, Keckes J, Fratzl P, Stanzl-Tschegg S (2004) Structure-function relationships of four compression wood types: micromechanical properties at the tissue and fibre level. Trees 18(4):480. https://doi.org/10.1007/s00468-004-0334-y

CEN (2003) Moisture content of a piece of sawn timber—Part 1: determination by oven dry method

Dahl KB, Malo KA (2009) Nonlinear shear properties of spruce softwood: experimental results. Wood Sci Technol 43(7–8):539–558. https://doi.org/10.1007/s00226-009-0247-4

Derome D, Griffa M, Koebel M, Carmeliet J (2011) Hysteretic swelling of wood at cellular scale probed by phase-contrast X-ray tomography. J Struct Biol 173(1):180–190. https://doi.org/10.1016/j.jsb.2010.08.011

Dinwoodie JM (2017) Timber: its nature and behaviour, 2nd edn. CRC Press, London. https://doi.org/10.4324/9780203477878

Donaldson L (2008) Microfibril angle: measurement, variation and relationships—a review. IAWA J 29(4):345–386. https://doi.org/10.1163/22941932-90000192

Donaldson LA, Singh Adya P (2016) Chapter 6–reaction wood. In: Kim YS, Funada R, Singh AP (eds) Secondary xylem biology. Academic Press, New York, pp 93–110

Färber J, Lichtenegger HC, Reiterer A, Stanzl-Tschegg S, Fratzl P (2001) Cellulose microfibril angles in a spruce branch and mechanical implications. J Mater Sci 36:5087–5092. https://doi.org/10.1023/A:1012465005607

Florisson S, Hartwig M, Wohlert M, Gamstedt EK (2023) Microscopic computed tomography aided finite element modelling as a methodology to estimate hygroexpansion coefficients of wood: A case study on opposite and compression wood in softwood branches. Holzforschung 77(9):700–712. https://doi.org/10.1515/hf-2023-0014

Gardiner B, Barnett J, Saranpää P, Gril J (eds) (2014) The biology of reaction wood. Springer Series in Wood Science. Springer, Berlin, https://doi.org/10.1007/978-3-642-10814-3https://doi.org/10.1007/978-3-642-10814-3

Gurau L, Cionca M, Mansfield-Williams H, Sawyer G, Zeleniuc O (2008) Comparison of the mechanical properties of branch and stem wood for three species. Wood Fiber Sci 40(4):647–656

Harris JM (1977) Shrinkage and density of radiata pine compression wood in relation to its anatomy and mode of formation. NZ J Forest Sci 7(1):16

He H, Zhang C, Zhao X et al (2018) Allometric biomass equations for 12 tree species in coniferous and broadleaved mixed forests, Northeastern China. PLOS ONE 13(1):e0186226. https://doi.org/10.1371/journal.pone.0186226

Joffre T, Neagu RC, Bardage SL, Gamstedt EK et al (2014) Modelling of the hygroelastic behaviour of normal and compression wood tracheids. J Struct Biol 185(1):89–98. https://doi.org/10.1016/j.jsb.2013.10.014

Jungnikl K, Goebbels J, Burgert I, Fratzl P (2009) The role of material properties for the mechanical adaptation at branch junctions. Trees 23(3):605–610. https://doi.org/10.1007/s00468-008-0305-9

Keunecke D, Hering S, Niemz P (2008) Three-dimensional elastic behaviour of common yew and Norway spruce. Wood Sci Technol 42(8):633–647. https://doi.org/10.1007/s00226-008-0192-7

Leonardon M, Altaner CM, Vihermaa L, Jarvis MC (2010) Wood shrinkage: influence of anatomy, cell wall architecture, chemical composition and cambial age. Eur J Wood Prod 68(1):87–94. https://doi.org/10.1007/s00107-009-0355-8

Li X, Evans R, Gapare W, Yang X, Wu HX (2014) Characterizing compression wood formed in radiata pine branches. IAWA J 35(4):385–394. https://doi.org/10.1163/22941932-00000073

Müller U, Gindl W, Jeronimidis G (2006) Biomechanics of a branch—stem junction in softwood. Trees 20(5):643–648. https://doi.org/10.1007/s00468-006-0079-x

Olarescu AM, Lunguleasa A, Radulescu L (2022) Using deciduous branch wood and conifer spindle wood to manufacture panels with transverse structure. BioResources 17(4):6445–6463. https://doi.org/10.15376/biores.17.4.6445-6463

Perstorper M, Johansson M, Kliger R, Johansson G (2001) Distortion of Norway spruce timber. Holz Roh- Werkst 59:94–103. https://doi.org/10.1007/s001070050481

Purusatama BD, Febrianto F, Lee SH, Kim NH (2021) Physical and mechanical properties of reaction wood of tropical softwood species. Eur J Wood Prod 79(1):241–243. https://doi.org/10.1007/s00107-020-01602-0

Reiterer A, Jakob HF, StanzI-Tschegg SE, Fratzl P (1998) Spiral angle of elementary cellulose fibrils in cell walls of Picea abies determined by small-angle X-ray scattering. Wood Sci Technol 32:335–345

Schindelin J, Arganda-Carreras I, Frise E, Kaynig V, Longair M, Pietzsch T, Preibisch S, Rueden C, Saalfeld , Schmid B, Tinevez J, White DJ, Hartenstein V, Eliceiri K, Tomancak P, Cardona A (2012) Fiji: an open-source platform for biological-image analysis. Nat Methods 9(7):676–682. https://doi.org/10.1038/nmeth.2019

Simpson WT (1973) Predictig equilibrium moisture content of wood by mathematical models. Wood Fiber 5(1):41–49

Stanzl-Tschegg SE, Keunecke D, Tschegg EK (2011) Fracture tolerance of reaction wood (yew and spruce wood in the TR crack propagation system). J Mech Behav Biomed Mater 4(5):688–698. https://doi.org/10.1016/j.jmbbm.2010.11.010

Tarmian A, Azadfallah M (2009) Variation of cell features and chemical composition in spruce consisting of opposite, normal, and compression wood. BioResources 4:194–204. https://doi.org/10.15376/biores.4.1.194-204

Timell TE (1986) Compression wood in gymnosperms, 1st edn. Springer-Verlag, Berlin

Vorobyev A, Bjurhager I, Van Dijk NP, Gamstedt EK (2016) Effects of barrelling during axial compressive tests of cubic samples with isotropic, transversely isotropic and orthotropic elastic properties. Compos Sci Technol 137:1–8. https://doi.org/10.1016/j.compscitech.2016.10.015

Withers PJ, Bouman C, Carmignato S, Cnudde V, Grimaldi D, Hagen CK, Maire E, Manley M, Du Plessis A, Stock SR (2021) X-ray computed tomography. Nat Rev Methods Primers 1(1):18. https://doi.org/10.1038/s43586-021-00015-4

Zhan T, Lyu J, Eder M (2021) In situ observation of shrinking and swelling of normal and compression Chinese fir wood at the tissue, cell and cell wall level. Wood Sci Technol 55(5):1359–1377. https://doi.org/10.1007/s00226-021-01321-6

Zhang M, Chavan RR, Smith BG, McArdle MH, Harris PJ (2016) Tracheid cell-wall structures and locations of (1 → 4)-β-d-galactans and (1 → 3)-β-d-glucans in compression woods of radiata pine (Pinus radiata D. Don). BMC Plant Biol 16(1):194. https://doi.org/10.1186/s12870-016-0884-3